

Remote Sensing of Atmospheric Thermodynamics in the Tropics

Siri Jodha KHALSA

*Cooperative Institute for Research in Environmental Sciences,
University of Colorado,
Boulder, CO 80309 - U.S.A.*

1. Introduction.

Successful diagnosis and prognosis of coupling between the tropical oceans and global atmosphere requires knowledge of the thermodynamic state of the atmosphere. The horizontal and vertical distribution of heat and moisture is important in the evolution of cloud clusters and tropical cyclones, and it is tied to the redistribution of convection during El Nino events. The propagation of convection associated with the 30-60 day oscillation depends upon, among other things, the thermodynamic basic state of the atmosphere. The lower tropospheric temperature and humidity are important in determining the magnitude of the latent, sensible and longwave radiative fluxes at the air-sea interface. And, of course, moisture in the form of clouds is important in determining insolation and freshwater flux into the ocean. Owing to the poor coverage of the tropics by radiosonde stations, remote sensing from space is the only practical means of obtaining the required thermodynamic information over the broad regions of the tropical oceans.

I briefly review the principal satellite sensors that have been used to measure thermodynamical variables in the tropics and mention some of the studies that have been done with these instruments. I then describe work that has been done at CIRES with a gridded TOVS data set. This work encompasses studies of interannual (ENSO), intraseasonal (30-60 day), and high-frequency (synoptic) variability in the tropics. Finally, I discuss current and proposed methods of estimating latent and perhaps sensible heat fluxes using satellite data.

2. Previous and current satellites used to measure tropical thermodynamics.

In this review only instruments that are on polar orbiting platforms are discussed. Geostationary satellites have the advantage of being able to sample the same location on the earth many times in a day but at present only the U.S. geostationary satellites (GOES) have the multi-channel radiometers on them necessary for atmospheric sounding.

Remote sensing of atmospheric temperature and moisture is accomplished by measuring upwelling radiances at specific frequencies, either in the infrared or microwave portions of the spectrum. Among the first to work with remote sensing of atmospheric variables over the ocean were Prabhakara et al. (1979), who used data from the Infrared Interferometer Spectrometer, IRIS, on Nimbus-4 to map seasonal distributions of precipitable water vapor. Chang and Wilheit (1979) used data from Nimbus-5 to estimate water vapor, liquid water and surface wind speed. Grody et al. (1980) used data from the Scanning Microwave Spectrometer on Nimbus-6 to examine atmospheric water vapor over the tropical Pacific. Kidder and Shyu (1984) examined data from the same instrument for its potential use in forecasting tropical cyclone motion.

The two instruments with the longest history and greatest use in remote sensing of atmospheric variables are the scanning multi-channel microwave radiometer, SMMR,



F 30253

carried by the Nimbus-7 satellite, and the TIROS operational vertical sounder, TOVS, flown on the TIROS (now called NOAA) series of satellites.

SMMR measured microwave radiation at five frequencies from which a number of geophysical parameters could be derived. This data has been used to estimate sea surface temperature, ocean surface wind speed, total column water vapor, and liquid water or rainrate. Data are available from 1978 to 1986. Limitations of this instrument include low (250 km) horizontal resolution, incomplete sampling of the globe in a day, problems with shifting calibration, and the fact that no parameters could be derived within 600 km of land due to sidelobe contamination. Nominal rms errors are 1-1.5°C for SST, 1.5-2 m.s⁻¹ for wind speed, and 0.2 g.cm⁻² for precipitable water. (Gloersen et al., 1984)

Prabhakara et al. (1982) used SMMR data to estimate water vapor over the oceans. Chang et al. (1984) produced monthly maps of precipitable water from SMMR data. Prabhakara et al. (1985) examined variations in global water vapor distribution associated with El Nino.

Liu (1984) described a method to estimate surface latent heat flux using a bulk parametrization with SMMR data. He derived relationship between total column water vapor and surface-level humidity and used this in conjunction with SMMR-derived wind speed and surface temperature. In Liu (1988), monthly averages of latent heat flux for the period 1980 - 1983 were examined.

TOVS consists of three separate instruments: a 20 channel high-resolution infrared sounder (HIRS-2), a four channel microwave sounder (MSU), and a three channel stratospheric sounder (SSU). NOAA polar orbiters have carried a TOVS since 1979 with two normally in orbit, providing six hourly coverage of most points on the earth. Its primary mission is to provide sounding information for assimilation into numerical forecast models.

TOVS is a sounder, it gives the vertical distribution of temperature and moisture, albeit at a lower resolution than radiosondes. The effective horizontal resolution of the soundings was 250 km until 1986 when improvements in the retrieval techniques increased this to 50 km (the resolution of the instruments did not change, only the manner in which data from the instruments was processed). Moisture information is derived solely from the IR channels and is thus unavailable in completely cloudy situations although the microwave sounder gives temperature information under these circumstances. In comparisons with monthly tropical radiosonde data, TOVS had rms errors in the troposphere of roughly 0.5°C in temperature and 1-2 mm in precipitable water (Khalsa and Steiner, 1988)

Early applications of TOVS data to tropical studies focused on data from the FGGE. Cadet (1983) combined TOVS precipitable water data with ECMWF Level II-b humidity data in a study of the summer Indian monsoon. Reyes and Cadet (1988) used the same technique to examine horizontal moisture flux for the Mexican monsoon.

A new generation of microwave instruments is proving to be quite valuable in tropical studies. These are the Special Sensor Microwave Imager, SSM/I, and Special Sensor Microwave, Temperature, SSM/T, aboard the Defense Meteorological Satellite Program (DMSP) polar orbiters.

The SSM/I, a seven channel, four frequency, linearly polarized microwave radiometer, can measure a number of atmospheric, oceanographic and land parameters with a nominal resolution of 25 km. It is currently flying on the F8 satellite which has a 6:10 local ascending node equatorial crossing time. The 1400 km wide conical scan pattern and 102 minute orbital period requires at least 2.5 days for complete coverage in the tropics. Surface wind speed and total column water vapor content can be derived under cloudy conditions but not under regions of heavy rain (drop sizes greater than 100 μm). Where it is raining, cloud liquid water and rainrate can be derived. Evaluations of instrument accuracy place rms errors in wind speed at approximately 2 m s⁻¹ (Goodberlet, 1989), precipitable water at 4 mm (Alishouse, et al., 1989a), and cloud liquid water at 0.02 Kg m⁻² (Alishouse et al., 1989b). SMMR cannot resolve wind speeds below 3 m s⁻¹.

The SSM/T is a seven channel temperature sounder with a resolution of 174 km at nadir. It is currently flying on both the F7 and F8 DMSP satellites which both having morning ascending equatorial crossing times. Sounding products are being produced and archived by the National Environmental Satellite, Data, and Information Service, NESDIS. With a 1600 km wide, cross-track scan, a two satellite system is capable of providing nearly complete global coverage in a 24 hour period, producing 18,900 views per day. Comparisons with tropical radiosonde data gives rms errors in the 2-3°C range (Maiden et al., 1989).

Data from the SSM/I and SSM/T will be part of the program that we are proposing for remote sensing of latent and sensible heat flux. This will be discussed in Section 4.

3. Studies with TOVS.

The archived TOVS product has been obtained by CIRES from NESDIS for the years 1981-1988. Slightly over six years (October 1981 - December 1987) of data have been interpolated onto daily 5° latitude x 5° longitude grids. The gridded data include seven levels of temperature up to 100 mb (stratospheric data are not included) and 3 levels of precipitable water up to 300 mb.

The first use of TOVS data at CIRES was in a study of changes in the thermodynamic structure of the eastern Pacific troposphere during the 1982-83 El Nino (Garcia et al., 1986). TOVS data helped establish that the lower troposphere in the eastern Pacific became warm and moist several months prior to the arrival of deep convection.

Monthly averages of SST, HRC (a proxy for deep convection) and low-level precipitable water from TOVS for the period 1982 - 1985 were examined for the tropical equatorial Pacific in Steiner and Khalsa (1987). Fig. 1 shows the longitudinal variation in the correlation between these three variables. El Nino-induced variability in the eastern Pacific is responsible for a high correlation between all three variables there. West of 160°W the correlation between HRC and SST falls off rapidly. The only correlation that remains significant at the 95% level out to 150°E is that between low-level precipitable water (LLPW) and HRC. This implies that over the western Pacific, changes in convection on monthly time scales are more closely tied to changes in moisture supply, perhaps related to low-level wind convergence, than to sea surface temperature.

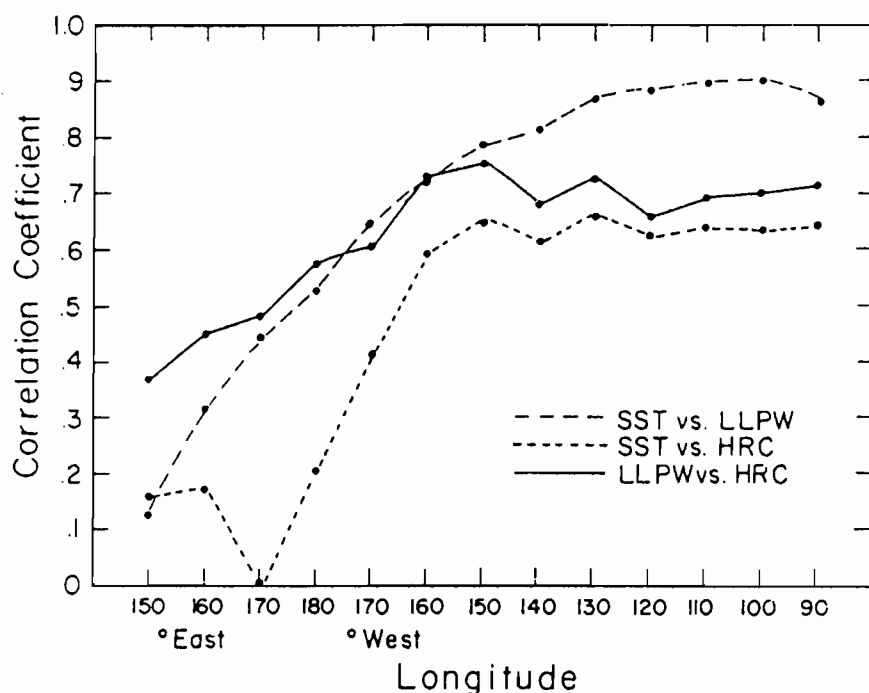


Fig.1. Simple correlation coefficients between sea surface temperature, low-level precipitable water and highly reflective cloud as a function of longitude.

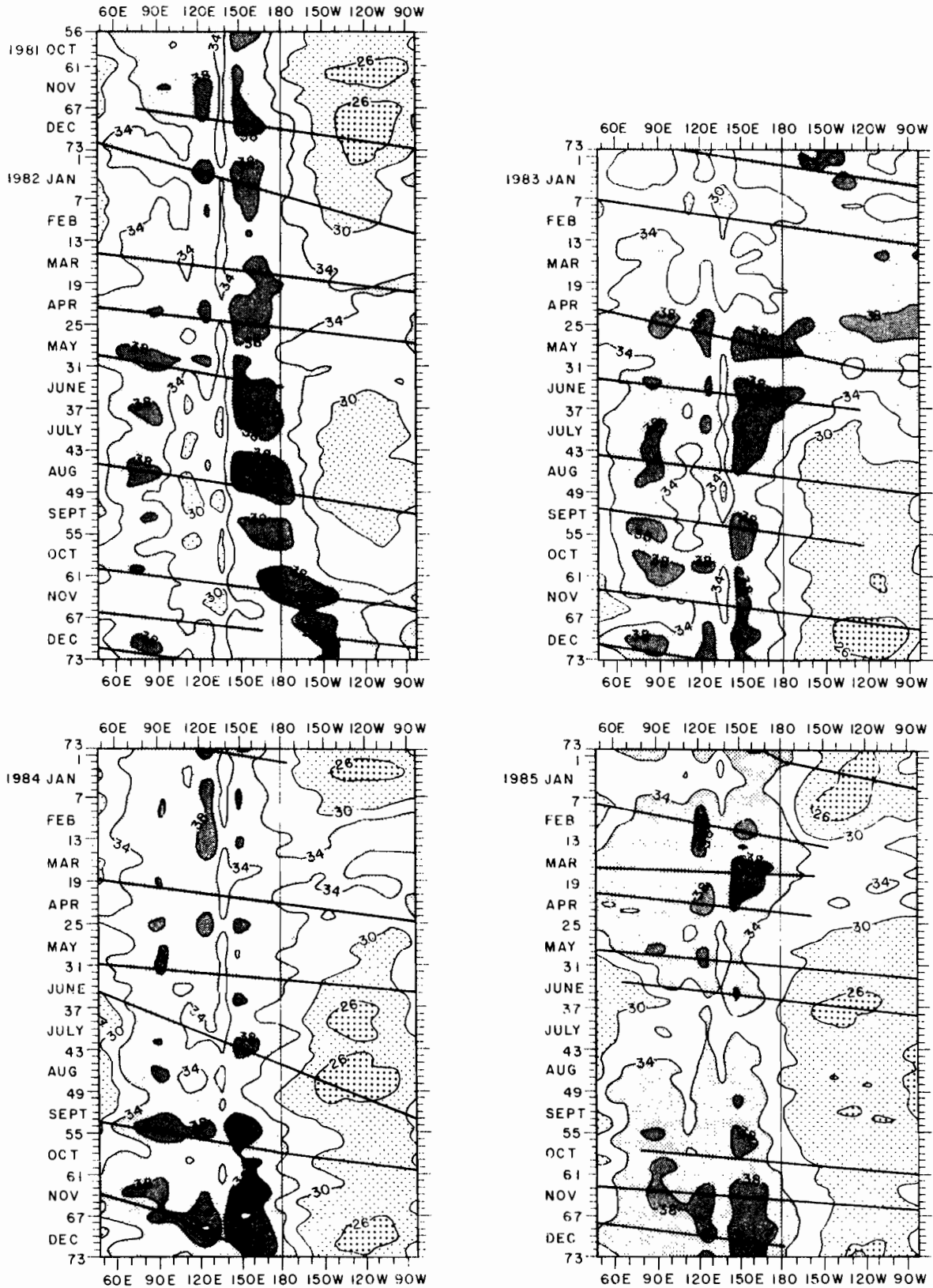


Fig.2. Time-longitude diagram of precipitable water (1000-700 mb) in millimeters for the 0°-5°S strip across the Indian and Pacific oceans from 3 October 1981 through 31 December 1985. Data are 5-day, 5° averages. Bold lines on the plot indicate axes of minima in filtered 250 mb velocity potential.

TOVS has proved valuable in studies of tropical phenomena on shorter time scales as well. Fig. 2 shows a time-longitude diagram of LLPW at 2.5°S latitude in the Indian and Pacific oceans for the period October 1981 through December 1985. In addition to the major changes in moisture distribution during the 1982-83 El Nino, higher frequency variations are evident. Superimposed on the plot are axes of filtered 250 mb velocity potential showing propagating 30-60 day oscillations. It will be noted that in most cases where there is an eastward extension of the 38 mm contour of LLPW there is a coincident passage of a 30-60 day wave.

In a case study of a 30-60 day oscillation (Weickmann et al., 1989, see also Weickmann and Khalsa, this volume), TOVS revealed that an increase in low-level moisture preceded the eastward movement of the bulk of convection from the Indian ocean to near the dateline (Fig. 3). This moisture increase coincided with strengthened easterlies and enhanced convergence (Steiner, 1989).

Low level moisture represents only part of the thermodynamic conditions that determine the potential for deep convection. A stability index, representing the buoyant forcing on a low level parcel when lifted to the middle troposphere, has been derived for use with TOVS data. This stability index is expressed as:

$$SI = \Theta_{es}(700-500 \text{ mb}) - \Theta_e(1000-850 \text{ mb})$$

where Θ_e (Θ_{es}) is the (saturated) equivalent potential temperature. Because of the coarse vertical resolution of the operational TOVS product this measure is not perfect. However, comparisons with in situ data show that SI is usually a good indicator of static stability in the tropics (Khalsa, 1989). Because of large diurnal changes in stability over continents, current investigations are limited to oceanic areas.

Five day, non-overlapping averages (pentads) were computed for the period of record. The annual cycle was removed by subtraction of the long-term (6 year) pentad mean at each grid point. To study interannual variability, a 12 month (73 pentad) running mean was computed. To isolate intraseasonal variability, a band pass filter with half power points at 28 and 72 days was applied to the data. The outgoing longwave radiation (OLR) data set, which measures cloud top temperatures, is used as a proxy for deep convection.

The character of the time variability in SI for the grid point at 2.5°S, 172.5°E is shown in Fig. 4. In this example the annual cycle has not been removed. Variations across a broad range of time scales are evident. In the latter half of 1982 stability was low and quasi-periodic fluctuations with a 40-50 day time scale are seen. These oscillations were followed by a rapid change to stable conditions in early 1983. The cause of this change was the movement of the warmest waters and bulk of convection to east of the dateline during El Nino. The lowest values of stability occurred in 1987, another El Nino year, and were followed, as in 1983, by a rapid change to large values of SI, at the end of the record.

The 1981-1987 December through February means of SI and OLR are shown in Fig.5. There is a good correspondence of negative stability index and low OLR (high clouds, deep convection) in the western Pacific/Indonesian region and in the South Pacific Convergence Zone. Lower SI values in the eastern Pacific and Atlantic Intertropical Convergence Zones are also evident. High values of SI off the western coasts of the continents, where oceanic upwelling produces stable conditions, are also clearly seen.

The variances of Θ_{e1} (TOVS level 1 = 1000-850 mb) and Θ_{es3} (level 3 = 700-500 mb) for the intraseasonal (28-72 day) time scale are shown in Fig.6. The greatest variability in these quantities occurs at latitudes poleward of 20° where midlatitude waves produce fluctuations in temperature throughout the troposphere. When Fig.6 and Fig. 7, which shows the intraseasonal variance in SI, are compared it is evident that the large fluctuations in the subtropics generally occur simultaneously at most levels in the troposphere, resulting in a small net effect on SI. In contrast to Θ_{e1} and Θ_{es3} , the maxima in SI variance occur in

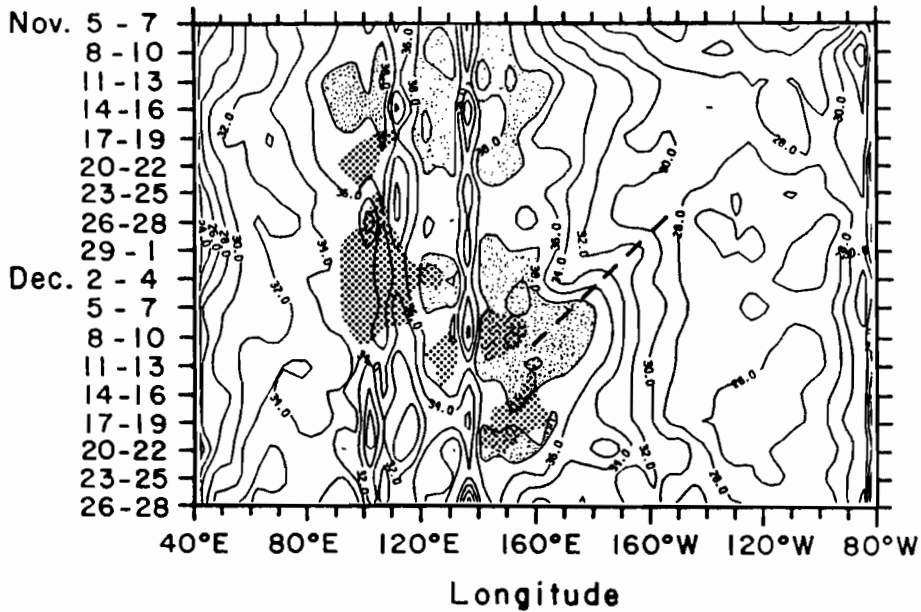


Fig.3. Time-longitude diagram of 3-day averaged low-level precipitable water averaged from 2.5°N-2.5°S for 5-7 November 1981 through 26-28 December 1981. The contour interval is 2 mm and values greater than 38 mm and stippled. Dotted areas indicate values of OLR < 180 $W.m^{-2}$.

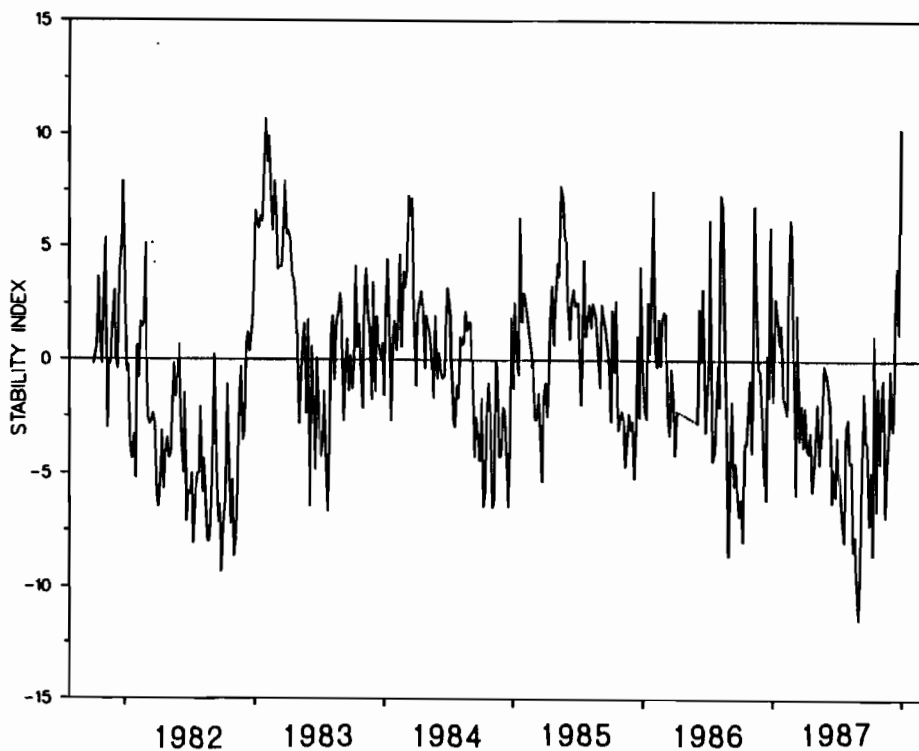


Fig.4. Time series of the stability index at 2.5°S, 172.5°E for the period of record.

specific regions known to be affected by the Madden and Julian (30-60 day) oscillation, i.e. the Indian and western Pacific oceans. The maximum off the coast of east Asia may arise from cold surges coming off the Asian land mass. These events have been shown to be coupled to the Madden and Julian Oscillation (Weickmann et al., 1989).

What is unusual about Fig. 7 is that SI variance in the equatorial Indian and far western Pacific oceans is relatively small. This is a region of strong intraseasonal variance in convection as shown in Fig. 8 (Lau and Chan, 1988). This is also the region of warmest sea surface temperatures. Over these very warm waters the stability is always low and the changes in stability associated with the onset and cessation of convection are small.

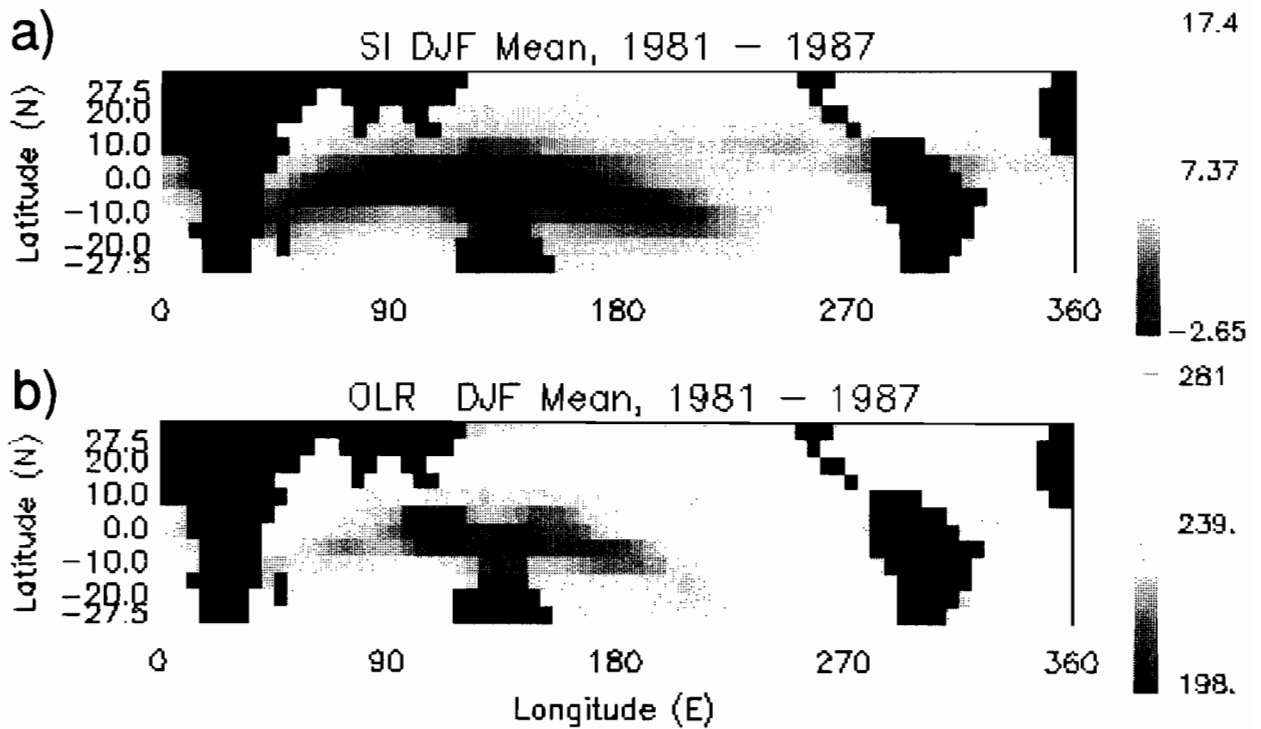


Fig.5. December-February means of a) stability index, and b) outgoing longwave radiation, for the global tropics ($\pm 30^\circ$ latitude) from the years 1971-1987.

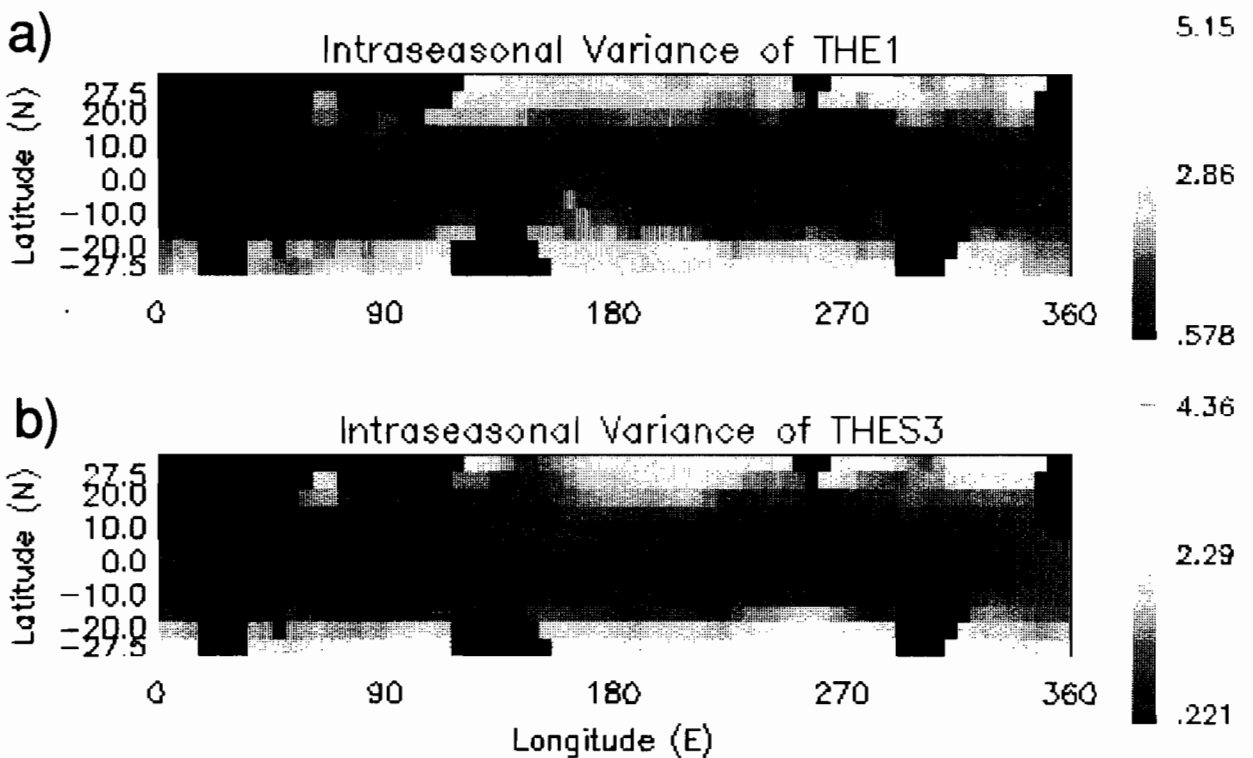


Fig.6. Intraseasonal variance of a) Θ_e (1000-850 mb), and b) Θ_{es} (700-500 mb) from the period October 1981 through December 1987.

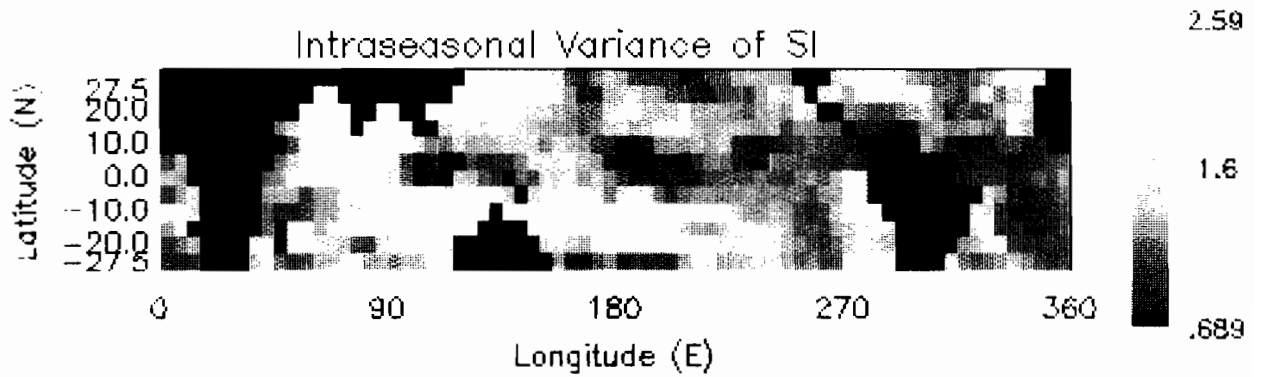


Fig.7. Same as for Fig.6 but for the stability index.

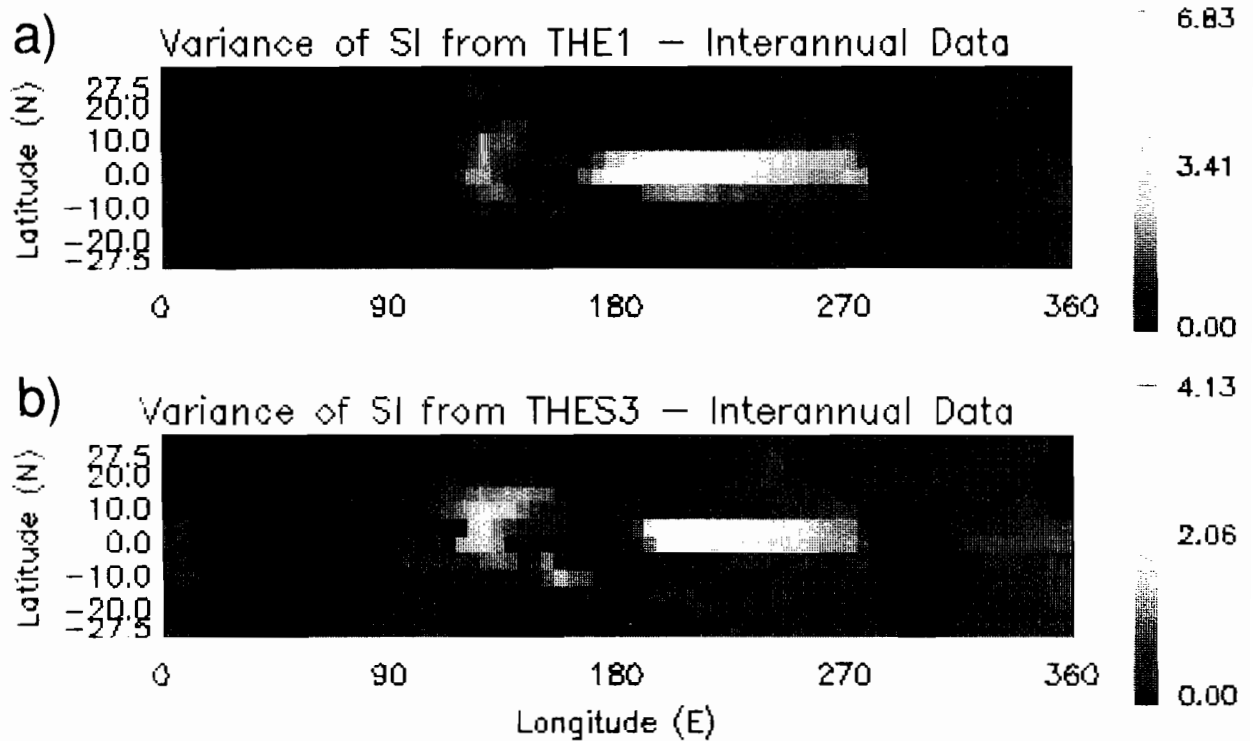


Fig.9. Magnitude of the interannual variance of the stability index explained by a) Θ_e (1000-850 mb), and b) Θ_{es} (700-500 mb).

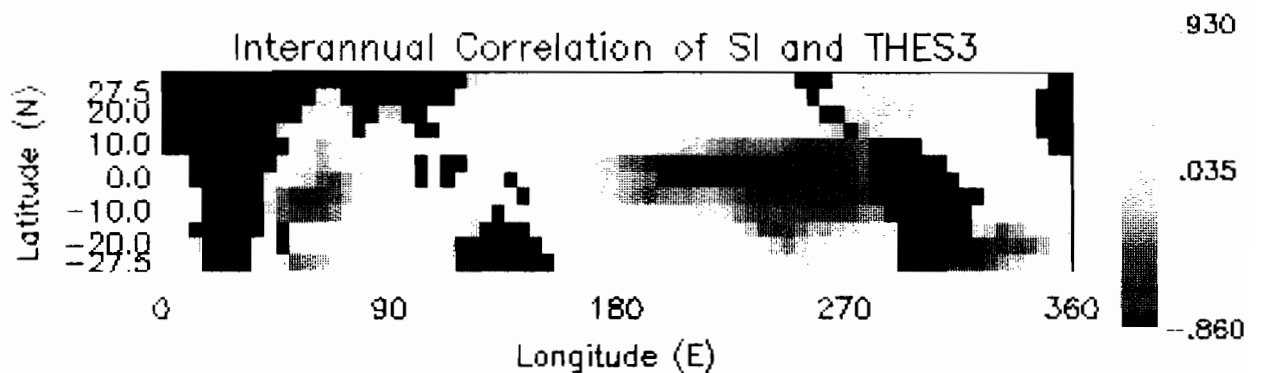


Fig.10. Correlation between the stability index and Θ_{es} (700-500 mb) for interannual time scales.

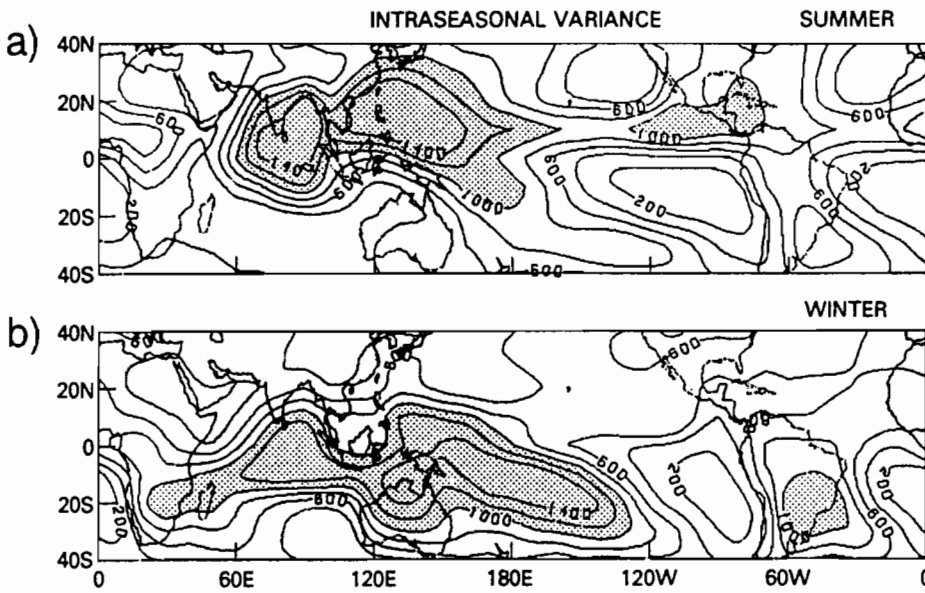


Fig.8. Intraseasonal variance of OLR for a) northern summer (May-October) and winter (November-April) from Lau and Chan (1988).

Interannual variance during the period of record is dominated by the 1982-83 El Nino. In Fig. 9 the magnitudes of the variance in SI that are produced by Θ_{e1} and Θ_{es3} (defined as the product of the variance in SI and the square of the correlation coefficient between SI and Θ_{e1} or Θ_{es3}) are shown. The largest variance in SI occurs where the sea surface temperature (SST) anomaly during El Nino is greatest. In the Indonesian region the magnitude of the contribution from Θ_{es3} , compared with the central Pacific maximum, is greater than that from Θ_{e1} . In other words, the warming of the middle troposphere in the Indonesian region contributes at least as much to the stabilization of the atmosphere during El Nino as low level drying. Fig. 10 shows the correlation of SI and Θ_{es3} . Negative values over the central and eastern Pacific Ocean mean that there the tendency for stabilization due to middle troposphere warming is completely overwhelmed by the destabilization produced by the warming and moistening of the lower layers due to SST anomalies.

4. Remote sensing of latent and sensible heat flux.

The method proposed by Liu (1984) to estimate surface latent heat flux from space relies on an empirical relationship between total column water vapor, W , and specific humidity, Q , at some level near the surface. This relationship is based on monthly mean radiosonde data. Its validity on shorter time scales is questionable. As an example, Fig. 11a shows the mixing ratio deviation for various stages of a tropical cloud cluster development derived from a large number of radiosonde stations in the western Pacific (Lee, 1986). Deviations of greater than 2 g.kg^{-1} occur in the middle troposphere while at the surface the deviations are less than 0.5 g.kg^{-1} . Clearly, in this case changes in total column water vapor are not simply related to changes in surface mixing ratio. The corresponding deviations in atmospheric temperature are shown in Fig. 11b.

The variability in the vertical distribution of heat and water vapor on synoptic time scales poses a challenge in any effort at remotely sensing surface heat fluxes. To the degree that the atmospheric perturbations associated with convective disturbances, such as those represented in Fig. 11, can be classified, it may be possible to define a set of Q - W relationships that could be used in a bulk parametrization formulation. This set of reference profiles would also be used in an improved retrieval algorithm for SSM/T.

If for each perturbation temperature profile in this reference set there is an associated perturbation humidity profile, then SSM/T could be used to identify the reference

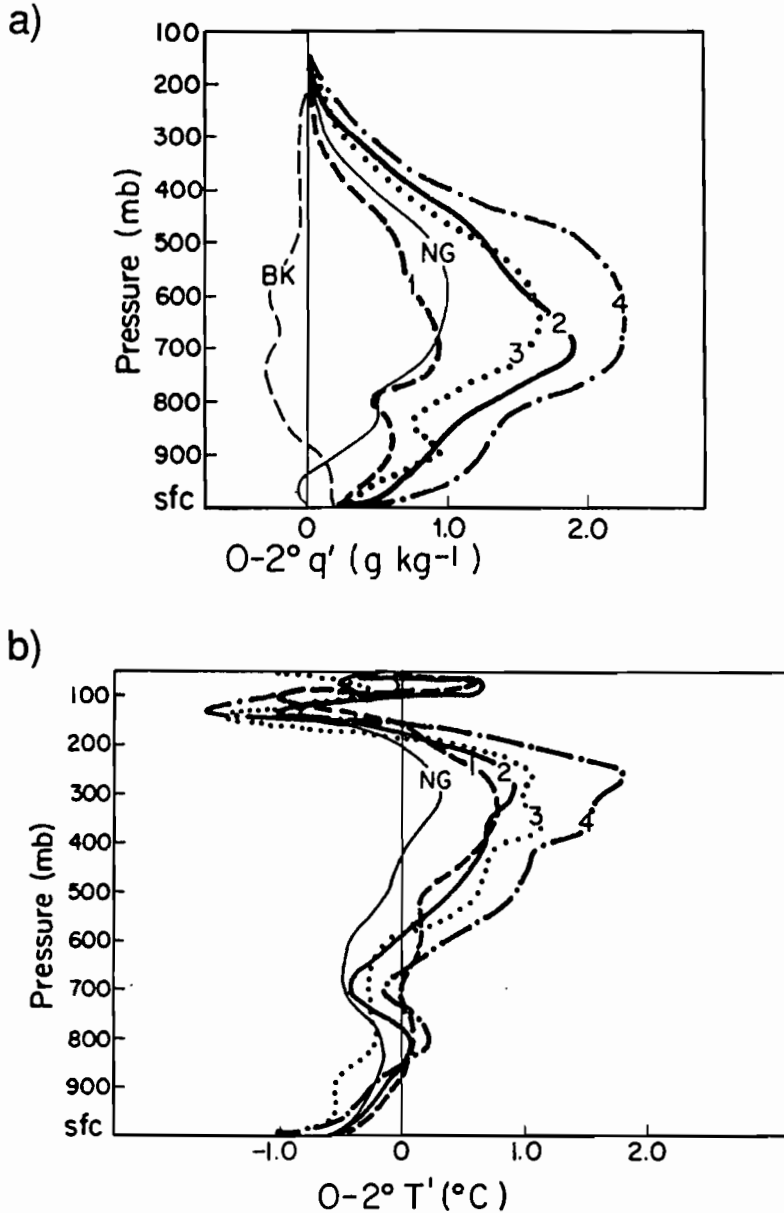


Fig.11. Deviations in the vertical profiles of a) mixing ratio and b) temperature for 4 stages of a developing tropical cyclone, the non-genesis (NG) cloud cluster case and the background (BK) composite. All profiles derived from a large number of island radiosonde reports.

Fig.11. Deviations in the vertical profiles of a) mixing ratio and b) temperature for 4 stages of a developing tropical cyclone, the non-genesis (NG) cloud cluster case and the background (BK) composite. All profiles derived from a large number of island radiosonde reports.

temperature profile and SSM/I could be used to scale the reference humidity profile to give the corresponding total column water vapor. The Q-W relationship for this humidity profile would then give the surface mixing ratio to be used in the bulk formulation. Wind speed would be obtained from SSM/I but SST would have to be obtained from another source, probably AVHRR.

Remote sensing of sensible heat flux can be more problematic, especially in the warm pool region where the air-sea temperature difference is small. However, as shown by Fig. 11b, surface air is cooler in disturbed conditions, probably due to convectively driven downdrafts, increasing air-sea temperature differences and sensible heat flux. It may be possible to parametrize the sensible heat flux for these circumstances using the method proposed above for latent heat flux. This might capture a large fraction of the time-averaged flux. The contribution from undisturbed periods could be estimated from climatology.

The proposed method for estimating fluxes depends on the identification of appropriate

perturbation temperature and humidity profiles from which near-surface values can be derived for use in bulk parametrization formulae. Satellite sounders do not work under conditions of heavy rain and so cannot be used for this purpose. It may be possible, however, to associate thermodynamic profiles, or more directly, near-surface temperature and humidity perturbations, with a given convective state as identified by visible and broad band IR imagery. The stages of evolution of a convective cloud cluster may be characterized by texture and other higher order spatial moments derived from imagery. The magnitudes of the perturbations might be related to the coldest cloud tops identified by IR emissions.

5. Conclusions.

Remote sensing can add greatly to our knowledge of the thermodynamic processes governing ocean-atmosphere coupling. New approaches to remote sensing of air-sea heat fluxes await development and testing with field programs such as TOGA COARE.

REFERENCES

- Alishouse, J. C., S. Snyder and J. Vongsathorn, 1989a: Determination of total precipitable water in the tropics from the SSM/I. *Preprints of the Fourth Conference on Satellite Meteorology and Oceanography*, May 16-19, San Diego, Calif., American Meteorological Society, pp. 221-223.
- Alishouse, J. C., C. Swift, C. Ruf, S. Snyder and J. Vongsathorn, 1989b: Determinations of cloud liquid water in the tropics from the SSM/I. *Preprints of the Fourth Conference on Satellite Meteorology and Oceanography*, May 16-19, San Diego, Calif., American Meteorological Society, pp. 187-189.
- Cadet, D. L., 1983: Mean fields of precipitable water over the Indian Ocean during the 1979 summer monsoon from TIROS-N soundings and FGGE data. *Tellus*, **35B**, 329-345.
- Chang, A. T. C., and T. T. Wilheit, 1979: Remote sensing of atmospheric water vapor, liquid water, and wind speed at the ocean surface by passive microwave techniques from Nimbus 5 satellite. *Radio Sci.*, **14**, 793-803.
- Chang, H. D., P. H. Hwang, T. T. Wilheit, A. T. C. Chang, D. H. Staelin and P. W. Rosenkrans, 1984: Monthly distributions of precipitable water from the Nimbus 7 SMMR data. *J. Geophys. Res.*, **89**, 5328-5334.
- Garcia, O., S. J. S. Khalsa and E. Steiner, 1986: Atmospheric characteristics of the eastern equatorial Pacific during the 1982-83 El Nino, deduced from satellite and aircraft measurements. *J. Geophys. Res.*, **91**, 13,217-13,231.
- Gloersen, P., D. J. Cavalieri, A. T. C. Chang, T. T. Wilheit, W. J. Campbell, O. M. Joannessen, K. B. Katsaros, K. F. Kunzi, D. B. Ross, D. Staelin, E. P. L. Windsor, F. T. Barath, P. Gudmandsen, E. Langham and R. O. Ramseier, 1984: A summary of results from the first Nimbus 7 SMMR observations. *J. Geophys. Res.*, **89**, 5335-5344.
- Goodberlet, M. A., 1989: Remote sensing of ocean surface winds with the Special Sensor Microwave/Imager (SSM/I). *Preprints of the Fourth Conference on Satellite Meteorology and Oceanography*, May 16-19, San Diego, Calif., American Meteorological Society, pp. J42-45.
- Grody, N. C., A. Gruber and W. C. Chen, 1980: Atmospheric water vapor content over the tropical Pacific derived from the Nimbus-6 Scanning Microwave Spectrometer. *J. Appl. Meteor.*, **19**, 986-996.

- Khalsa, S. J. S. and E. J. Steiner, 1988: A TOVS data set for study of the tropical atmosphere. *J. Appl. Meteor.*, **27**, 851-862.
- Khalsa, S. J. S., 1989: Atmospheric stability over the tropical oceans, derived from TOVS. *J. Appl. Meteor.*, August issue.
- Kidder, S. Q. and K. Shyu, 1984: On the potential use of satellite sounder data in forecasting tropical cyclone motion. *Mon. Wea. Rev.*, **112**, 1977-1984.
- Lau, K. M. and P. H. Chan, 1988: Intraseasonal and interannual variations of tropical convection: a possible link between the 40-50 day oscillation and ENSO ? *J. Atmos. Sci.*, **45**, 506-521.
- Lee, C.-S., 1986: An observational study of tropical cloud cluster evolution and cyclogenesis in the western north Pacific. Dept. Atmos. Sci. Paper No. 403, Colorado State University, Fort Collins, Colorado, 80523.
- Liu, W. T., 1984: Determination of monthly mean humidity in the atmospheric surface layer over oceans from satellite data. *J. Phys. Oceanogr.*, **14**, 1451-1457.
- Liu, W. T., 1988: Moisture and latent heat flux variabilities in the tropical Pacific derived from satellite data. *J. Geophys. Res.*, **93**, 6749-6760.
- Maiden, M. E., M. V. Piepgrass, D. R. Donahue, M. Sylva, H. F. Drahos, Jr., 1989: Atmospheric temperature retrieval from satellite microwave measurements. *Preprints of the Fourth Conference on Satellite Meteorology and Oceanography*, May 16-19, San Diego, Calif., American Meteorological Society, pp. 204-207.
- Prabhakara, C., G. Dalu, R. C. Lo and N. R. Nath, 1979: Remote sensing of seasonal distribution of precipitable water over the oceans and the inference of boundary layer structure. *Mon. Wea. Rev.*, **107**, 1388-1401.
- Prabhakara, C., H. D. Chang and A. T. C. Chang, 1982: Remote sensing of precipitable water over the oceans from Nimbus 7 microwave measurements. *J. Appl. Meteor.*, **21**, 59-68.
- Prabhakara, C., D. A. Short and B. E. Vollmer, 1985: El Nino and atmospheric water vapor observations from Nimbus 7 SMMR. *J. Climate Appl. Meteor.*, **24**, 1311-1324.
- Reyes, S. and D. L. Cadet, 1988: The southwest branch of the North American monsoon during summer 1979. *Mon. Wea. Rev.*, **116**, 1175-1187.
- Steiner, E. J. and S. J. S. Khalsa, 1987: Sea surface temperature, low-level moisture, and convection in the tropical Pacific, 1982-1985. *J. Geophys. Res.*, **92**, 14,217-14,224.
- Steiner, E. J., 1989: Moisture convergence during a convective flare-up in the tropics. *Preprints of the Fourth Conference on Satellite Meteorology and Oceanography*, May 16-19, San Diego, Calif., American Meteorological Society, pp. 154-157.
- Weickmann, K. M., S. J. S. Khalsa and E. J. Steiner, 1989: The shift of convection from the Indian Ocean to the western Pacific Ocean during a 30-60 day oscillation. *Mon. Wea. Rev.*, in review.

**WESTERN PACIFIC INTERNATIONAL MEETING
AND WORKSHOP ON TOGA COARE**

Nouméa, New Caledonia

May 24-30, 1989

PROCEEDINGS

edited by

Joël Picaut *

Roger Lukas **

Thierry Delcroix *

* ORSTOM, Nouméa, New Caledonia

** JIMAR, University of Hawaii, U.S.A.

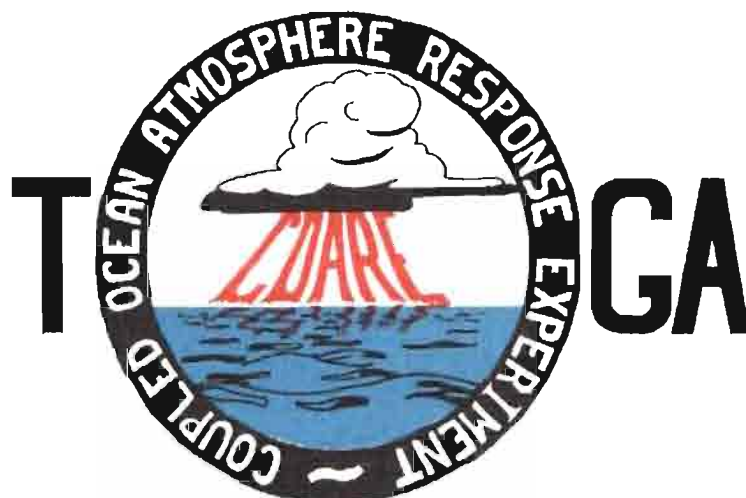


TABLE OF CONTENTS

ABSTRACT	i
RESUME	iii
ACKNOWLEDGMENTS	vi
INTRODUCTION	
1. Motivation	1
2. Structure	2
LIST OF PARTICIPANTS	5
AGENDA	7
WORKSHOP REPORT	
1. Introduction	19
2. Working group discussions, recommendations, and plans	20
a. Air-Sea Fluxes and Boundary Layer Processes	20
b. Regional Scale Atmospheric Circulation and Waves	24
c. Regional Scale Oceanic Circulation and Waves	30
3. Related programs	35
a. NASA Ocean Processes and Satellite Missions	35
b. Tropical Rainfall Measuring Mission	37
c. Typhoon Motion Program	39
d. World Ocean Circulation Experiment	39
4. Presentations on related technology	40
5. National reports	40
6. Meeting of the International Ad Hoc Committee on TOGA COARE	40
APPENDIX: WORKSHOP RELATED PAPERS	
Robert A. Weller and David S. Hosom: Improved Meteorological Measurements from Buoys and Ships for the World Ocean Circulation Experiment	45
Peter H. Hildebrand: Flux Measurement using Aircraft and Radars	57
Walter F. Dabberdt, Hale Cole, K. Gage, W. Ecklund and W.L. Smith: Determination of Boundary-Layer Fluxes with an Integrated Sounding System	81

MEETING COLLECTED PAPERS

WATER MASSES, SEA SURFACE TOPOGRAPHY, AND CIRCULATION

Klaus Wyrtki: Some Thoughts about the West Pacific Warm Pool	99
Jean René Donguy, Gary Meyers, and Eric Lindstrom: Comparison of the Results of two West Pacific Oceanographic Expeditions FOC (1971) and WEPOCS (1985-86)	111
Dunxin Hu, and Maochang Cui: The Western Boundary Current in the Far Western Pacific Ocean	123
Peter Hacker, Eric Firing, Roger Lukas, Philipp L. Richardson, and Curtis A. Collins: Observations of the Low-latitude Western Boundary Circulation in the Pacific during WEPOCS III	135
Stephen P. Murray, John Kindle, Dharma Arief, and Harley Hurlburt: Comparison of Observations and Numerical Model Results in the Indonesian Throughflow Region	145
Christian Henin: Thermohaline Structure Variability along 165°E in the Western Tropical Pacific Ocean (January 1984 - January 1989)	155
David J. Webb, and Brian A. King: Preliminary Results from Charles Darwin Cruise 34A in the Western Equatorial Pacific	165
Warren B. White, Nicholas Graham, and Chang-Kou Tai: Reflection of Annual Rossby Waves at The Maritime Western Boundary of the Tropical Pacific	173
William S. Kessler: Observations of Long Rossby Waves in the Northern Tropical Pacific	185
Eric Firing, and Jiang Songnian: Variable Currents in the Western Pacific Measured During the US/PRC Bilateral Air-Sea Interaction Program and WEPOCS	205
John S. Godfrey, and A. Weaver: Why are there Such Strong Steric Height Gradients off Western Australia ?	215
John M. Toole, R.C. Millard, Z. Wang, and S. Pu: Observations of the Pacific North Equatorial Current Bifurcation at the Philippine Coast	223

EL NINO/SOUTHERN OSCILLATION 1986-87

Gary Meyers, Rick Bailey, Eric Lindstrom, and Helen Phillips: Air/Sea Interaction in the Western Tropical Pacific Ocean during 1982/83 and 1986/87	229
Laury Miller, and Robert Cheney: GEOSAT Observations of Sea Level in the Tropical Pacific and Indian Oceans during the 1986-87 El Nino Event	247
Thierry Delcroix, Gérard Eldin, and Joël Picaut: GEOSAT Sea Level Anomalies in the Western Equatorial Pacific during the 1986-87 El Nino, Elucidated as Equatorial Kelvin and Rossby Waves	259
Gérard Eldin, and Thierry Delcroix: Vertical Thermal Structure Variability along 165°E during the 1986-87 ENSO Event	269
Michael J. McPhaden: On the Relationship between Winds and Upper Ocean Temperature Variability in the Western Equatorial Pacific	283

John S. Godfrey, K. Ridgway, Gary Meyers, and Rick Bailey: Sea Level and Thermal Response to the 1986-87 ENSO Event in the Far Western Pacific	291
Joël Picaut, Bruno Camusat, Thierry Delcroix, Michael J. McPhaden, and Antonio J. Busalacchi: Surface Equatorial Flow Anomalies in the Pacific Ocean during the 1986-87 ENSO using GEOSAT Altimeter Data	301

THEORETICAL AND MODELING STUDIES OF ENSO AND RELATED PROCESSES

Julian P. McCreary, Jr.: An Overview of Coupled Ocean-Atmosphere Models of El Nino and the Southern Oscillation	313
Kensuke Takeuchi: On Warm Rossby Waves and their Relations to ENSO Events	329
Yves du Penhoat, and Mark A. Cane: Effect of Low Latitude Western Boundary Gaps on the Reflection of Equatorial Motions	335
Harley Hurlburt, John Kindle, E. Joseph Metzger, and Alan Wallcraft: Results from a Global Ocean Model in the Western Tropical Pacific	343
John C. Kindle, Harley E. Hurlburt, and E. Joseph Metzger: On the Seasonal and Interannual Variability of the Pacific to Indian Ocean Throughflow	355
Antonio J. Busalacchi, Michael J. McPhaden, Joël Picaut, and Scott Springer: Uncertainties in Tropical Pacific Ocean Simulations: The Seasonal and Interannual Sea Level Response to Three Analyses of the Surface Wind Field	367
Stephen E. Zebiak: Intraseasonal Variability - A Critical Component of ENSO ?	379
Akimasa Sumi: Behavior of Convective Activity over the "Jovian-type" Aqua-Planet Experiments	389
Ka-Ming Lau: Dynamics of Multi-Scale Interactions Relevant to ENSO	397
Pecheng C. Chu and Roland W. Garwood, Jr.: Hydrological Effects on the Air-Ocean Coupled System	407
Sam F. Jacobellis, and Richard C.J. Somerville: A one Dimensional Coupled Air-Sea Model for Diagnostic Studies during TOGA-COARE	419
Allan J. Clarke: On the Reflection and Transmission of Low Frequency Energy at the Irregular Western Pacific Ocean Boundary - a Preliminary Report	423
Roland W. Garwood, Jr., Pecheng C. Chu, Peter Muller, and Niklas Schneider: Equatorial Entrainment Zone : the Diurnal Cycle	435
Peter R. Gent: A New Ocean GCM for Tropical Ocean and ENSO Studies	445
Wasito Hadi, and Nuraini: The Steady State Response of Indonesian Sea to a Steady Wind Field	451
Pedro Ripa: Instability Conditions and Energetics in the Equatorial Pacific	457
Lewis M. Rothstein: Mixed Layer Modelling in the Western Equatorial Pacific Ocean	465
Neville R. Smith: An Oceanic Subsurface Thermal Analysis Scheme with Objective Quality Control	475
Duane E. Stevens, Qi Hu, Graeme Stephens, and David Randall: The hydrological Cycle of the Intraseasonal Oscillation	485
Peter J. Webster, Hai-Ru Chang, and Chidong Zhang: Transmission Characteristics of the Dynamic Response to Episodic Forcing in the Warm Pool Regions of the Tropical Oceans	493

MOMENTUM, HEAT, AND MOISTURE FLUXES BETWEEN ATMOSPHERE AND OCEAN

W. Timothy Liu: An Overview of Bulk Parametrization and Remote Sensing of Latent Heat Flux in the Tropical Ocean	513
E. Frank Bradley, Peter A. Coppin, and John S. Godfrey: Measurements of Heat and Moisture Fluxes from the Western Tropical Pacific Ocean	523
Richard W. Reynolds, and Ants Leetmaa: Evaluation of NMC's Operational Surface Fluxes in the Tropical Pacific	535
Stanley P. Hayes, Michael J. McPhaden, John M. Wallace, and Joël Picaut: The Influence of Sea-Surface Temperature on Surface Wind in the Equatorial Pacific Ocean	543
T.D. Keenan, and Richard E. Carbone: A Preliminary Morphology of Precipitation Systems In Tropical Northern Australia	549
Phillip A. Arkin: Estimation of Large-Scale Oceanic Rainfall for TOGA	561
Catherine Gautier, and Robert Frouin: Surface Radiation Processes in the Tropical Pacific	571
Thierry Delcroix, and Christian Henin: Mechanisms of Subsurface Thermal Structure and Sea Surface Thermo-Haline Variabilities in the South Western Tropical Pacific during 1979-85 - A Preliminary Report	581
Greg. J. Holland, T.D. Keenan, and M.J. Manton: Observations from the Maritime Continent : Darwin, Australia	591
Roger Lukas: Observations of Air-Sea Interactions in the Western Pacific Warm Pool during WEPOCS	599
M. Nunez, and K. Michael: Satellite Derivation of Ocean-Atmosphere Heat Fluxes in a Tropical Environment	611

EMPIRICAL STUDIES OF ENSO AND SHORT-TERM CLIMATE VARIABILITY

Klaus M. Weickmann: Convection and Circulation Anomalies over the Oceanic Warm Pool during 1981-1982	623
Claire Perigaud: Instability Waves in the Tropical Pacific Observed with GEOSAT	637
Ryuichi Kawamura: Intraseasonal and Interannual Modes of Atmosphere-Ocean System Over the Tropical Western Pacific	649
David Gutzler, and Tamara M. Wood: Observed Structure of Convective Anomalies	659
Siri Jodha Khalsa: Remote Sensing of Atmospheric Thermodynamics in the Tropics	665
Bingrong Xu: Some Features of the Western Tropical Pacific: Surface Wind Field and its Influence on the Upper Ocean Thermal Structure	677
Bret A. Mullan: Influence of Southern Oscillation on New Zealand Weather	687
Kenneth S. Gage, Ben Basley, Warner Ecklund, D.A. Carter, and John R. McAfee: Wind Profiler Related Research in the Tropical Pacific	699
John Joseph Bates: Signature of a West Wind Convective Event in SSM/I Data	711
David S. Gutzler: Seasonal and Interannual Variability of the Madden-Julian Oscillation	723
Marie-Hélène Radenac: Fine Structure Variability in the Equatorial Western Pacific Ocean	735
George C. Reid, Kenneth S. Gage, and John R. McAfee: The Climatology of the Western Tropical Pacific: Analysis of the Radiosonde Data Base	741

Chung-Hsiung Sui, and Ka-Ming Lau: Multi-Scale Processes in the Equatorial Western Pacific	747
Stephen E. Zebiak: Diagnostic Studies of Pacific Surface Winds	757

MISCELLANEOUS

Rick J. Bailey, Helene E. Phillips, and Gary Meyers: Relevance to TOGA of Systematic XBT Errors	775
Jean Blanchot, Robert Le Borgne, Aubert Le Bouteiller, and Martine Rodier: ENSO Events and Consequences on Nutrient, Planktonic Biomass, and Production in the Western Tropical Pacific Ocean	785
Yves Dandonneau: Abnormal Bloom of Phytoplankton around 10°N in the Western Pacific during the 1982-83 ENSO	791
Cécile Dupouy: Sea Surface Chlorophyll Concentration in the South Western Tropical Pacific, as seen from NIMBUS Coastal Zone Color Scanner from 1979 to 1984 (New Caledonia and Vanuatu)	803
Michael Szabados, and Darren Wright: Field Evaluation of Real-Time XBT Systems	811
Pierre Rual: For a Better XBT Bathy-Message: Onboard Quality Control, plus a New Data Reduction Method	823